

## Helix Jump Mechanisms in Crystalline Isotactic Polypropylene

G. C. Rutledge\* and U. W. Suter

Institut für Polymere, Eidgenössische Technische Hochschule, CH-8092 Zürich, Switzerland

Received September 20, 1991; Revised Manuscript Received November 18, 1991

**ABSTRACT:** A proposed 120° helical jump process observed by 2D NMR spectroscopy to occur in the  $\alpha$ -crystalline form of isotactic polypropylene is analyzed by quasi-static methods of molecular modeling. Two competing mechanisms for describing the chain jump process, denoted herein as the *concerted-helix transition* and the *defect-translation transition*, are examined in terms of energetic stability and barriers to activation. Viable transitions of the concerted-helix type comprise a longitudinal translation of the polymer helix along its axis and a screw transition involving a 120° rotation accompanied by a  $c/3$  translation; of these two mechanisms, only the latter would account for the 2D NMR observations. Both mechanisms exhibit energy barriers of roughly 3.6 kcal/mol of propylene units, which increases linearly with the number of propylene units cooperating in the transition process. A viable crystalline defect described by a dispiration of the chain helix distributed over eight propylene units is identified having an energy of formation of 23.4 kcal/mol of defects, which is chain length independent. On this basis, it may be inferred that, in realistic lamellae of thicknesses in excess of 100 Å, the defect-translation mechanism represents the most likely mode of 120° helix jumps in the  $\alpha$ -crystalline modification of isotactic polypropylene.

## Introduction

The topic of molecular mobility in crystalline polymers has evolved in detail to the consideration of the atomic scale nature of relatively large-scale motions of atomic segments and how these may account for experimentally observed relaxation processes. Isotactic polypropylene (iPP) exhibits relaxation processes attributable to reorientational motion in the crystalline phase similar to those observed in polyethylene (PE).<sup>1</sup> Recently Schaefer et al.<sup>2</sup> reported two-dimensional solid-state NMR studies which presented evidence for a helical jump mechanism in the  $\alpha$ -modification of crystalline iPP, wherein the  $3_1$  helices appear to execute 120° rotations about their axes on the time scale of milliseconds. These measurements suggest a 120° rotational motion of the molecular helix about its axis but are insufficient to deduce the translational behavior or detailed mechanism of segmental reorientation within the crystal lattice.

A quasi-static molecular mechanics (MM) approach can provide suitable insight into the reorientation mechanism within such a crystal lattice. Questions concerning the energetic favorability of certain regular and irregular conformations in isolated chains or chain segments of PE and stereoregular vinyl polyalkanes have been addressed previously.<sup>3-6</sup> The response of isolated chain helices to imposed deformations has similarly been addressed.<sup>7</sup> The inclusion of defect structures in single chains or multichain lattices of PE is also amenable to analysis by MM methods: McCullough has considered the representation of localized defects in multichain structures.<sup>8</sup> Mansfield and Boyd<sup>9</sup> have simulated structures of packed docosyl-methylene chains as part of a study of defect structures in PE which could be responsible for the observed dielectric relaxation measurements. Reneker and Mazur<sup>10-12</sup> have simulated multichain structures composed of 60 CH<sub>2</sub> units per chain in order to further categorize the structure of local defects which may be incorporated into PE crystallites and have studied the translational mobility of these defects along the length of the polymer chain. Syi and Mansfield<sup>13</sup> combined rigid lattice packing energy maps with elastic rod approximations for molecular helices to

determine the energy requirements for solitary defect motion within several related polymers: polyethylene, isotactic polypropylene, syndiotactic polypropylene, and polystyrene. More recently, Bleha et al. have employed single-chain MM simulations of PE to explore the role played by conformational defects on mechanical response.<sup>14</sup>

The contributions of defects to mechanisms describing molecular motions and relaxation processes in polyolefin crystals remain a topic of discussion. In this paper, we apply the detailed MM methodology to the study of reorientational motion of iPP chains in the crystalline lattice ( $\alpha$ -modification) in both the concerted-helix-motion and defect-translation models, in an attempt to elucidate further the mechanism for the "helical jump" relaxation process in iPP and to help to clarify the conformational characteristics of the "elastic rod" description of the polymer chain.

## Model Description

**$\alpha$ -Modification.** The detailed analysis of conformational behavior of the polymer chain in the crystalline phase via MM requires interpretation at several levels of complexity. In the solid state, iPP itself may realize one or more of at least three crystalline modifications,<sup>15-17</sup> denoted  $\alpha$  (the predominant, monoclinic form),  $\beta$  (hexagonal), and  $\gamma$  (paracrystalline smectic); all three modifications exhibit the persistent  $3_1$  helix in left-handed and right-handed forms. Before proceeding to the analysis of relaxation mechanisms in the crystalline state of iPP, it is a first requisite to establish the validity of the model through analysis of the molecular representation of the basic single-chain and multichain structures in the absence of defects or disturbances. We are concerned here ultimately with the behavior of iPP chains in the predominant  $\alpha$ -modification of the crystalline solid state, first reported by Natta and Corradini.<sup>15</sup> The unit cell geometry of this crystalline modification is summarized in Table I. Subsequent work by Mencik<sup>18</sup> has pointed out the fact that the  $3_1$  helix of iPP lacks the necessary 2-fold symmetry axis for the  $C2/c$  space group and that in fact one must consider not only left-handed and right-handed helices but up and down orientations of these helices in the lattice as well, which led to the proposal of the  $P2_1/c$  space group for the  $\alpha$ -modification. The justification for the former

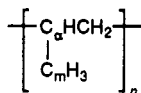
\* To whom all correspondence should be addressed at the Department of Chemical Engineering, Massachusetts Institute of Technology, Cambridge, MA 02139.

Table I  
Crystalline  $\alpha$ -Phase Unit Cell Description<sup>a</sup>

space group	C2/c
$a, b, c$ (Å)	6.65, 20.96, 6.50
$\beta$ (deg)	99.3
$(x_i, y_i, z_i)$	(0, $1/4$ , $1/2$ )

<sup>a</sup> From Natta and Corradini.<sup>15</sup>

Table II  
Chain Parametrization<sup>a</sup>



bond length (Å)	C-C	1.54
	C-H	1.10
bond angle (deg)	C-C $\alpha$ -C	114
	C $\alpha$ -C-C $\alpha$	114
	C-C $\alpha$ -C $\text{m}$ <sup>b</sup>	110
	C-C $\alpha$ -H	110
	C $\alpha$ -C-H	109
	C $\text{m}$ -C $\alpha$ -H <sup>b</sup>	110
	H-C $\text{m}$ -H <sup>c</sup>	109.5

		$r_i$ , Å	$\alpha_i$ , Å <sup>3</sup>	$N_i$
nonbonded potential	C	1.8	0.93	5
	H	1.3	0.42	0.9
	R <sup>d</sup> (=CH <sub>3</sub> )	2.0	1.77	7.0

<sup>a</sup> C $\alpha$  denotes the methine carbon, and C $\text{m}$  denotes the methyl carbon. <sup>b</sup> In the united methyl atom description, these values are used with C $\text{m}$  representing the methyl "atom" R. <sup>c</sup> This parameter is required only for the description in which the atoms of the methyl group are treated explicitly. <sup>d</sup> R refers to the "united methyl atom".

space group was based on the suggestion that both up- and down-oriented chains occur with equal frequency, such that there is no preferred orientation and that interchange of up- and down-oriented chains would not affect the unit cell dimensions. The latter  $\alpha$ -form, characterized by the regularity of up and down orientations of the chains and designated the  $\alpha_2$ -modification, is obtainable by annealing at high temperatures ( $T > 425$  K).<sup>19,20</sup> For simplicity, we have limited our calculations up to this point to considerations of the Natta-Corradini unit cell, designated the  $\alpha_1$ -modification, with the intimation that, at the scale of atomic packing, groups of like-oriented chains, whether up- or down-oriented, will exhibit the same behavior.

**Single Chain.** The isolated helix of iPP was initially studied using two models of the polymer chain. The first was the fully explicit description in which all atoms of the backbone and pendant methyl moieties are considered (including methyl group rotation about the carbon-carbon bond). A second, simpler description in which the methyl moieties are "collapsed" into spherical, "united methyl atoms", similar to the chain description employed by Theodorou and Suter<sup>21</sup> in their simulations of atactic polypropylene glasses, was also explored. Values for bond lengths and bond angles have been selected from crystallographic data appropriate to the  $\alpha$ -modification.<sup>15,18</sup> Previous investigations of the sensitivity of conformational minima to variations in bond angles have indicated that the latter may be reasonably treated as fixed parameters in the vicinity of the conformational energy minima.<sup>4</sup> The results reported here have all been obtained using the fixed bond length, fixed bond angle approximation; these values for the fixed parameters are given in Table II. An intrinsic 3-fold torsional potential of the form  $E_\phi = \frac{1}{2}k_\phi(1 - \cos 3\phi)$  was assigned to each skeletal C-C bond, with  $k_\phi$  equal to 2.8 kcal/mol;<sup>3</sup> Wright and Taylor have suggested that this additional torsional barrier potential is not

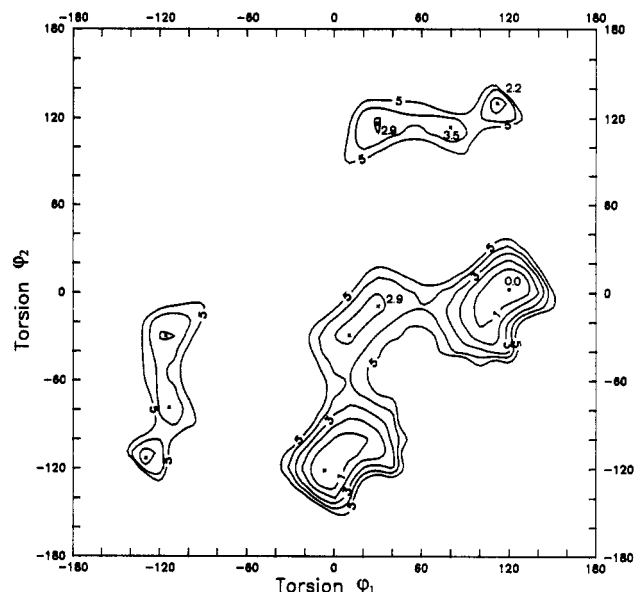


Figure 1. Conformational potential energy contour plot for helical conformations of a single chain of isotactic polypropylene where methyl groups have been represented as a single "united" atom. The 'x's mark the conformational minima for both right- and left-handed helices. Energy contour levels are shown for intervals of 1 kcal/mol up to 5 kcal/mol of repeat units.

required in order to simulate conformational behavior in the vicinity of the conformational energy minima.<sup>6</sup> In the force field employed here, however, we found this explicit torsional potential term necessary to account for the predominance of the  $3_1$  helix conformation. Nonbonded interactions between atoms separated by more than two bonds within a chain or between atoms in separate chains were computed using the Lennard-Jones 6-12 pair interaction  $E_{ij} = a_{ij}/r_{ij}^{12} - c_{ij}/r_{ij}^6$ . Parametrization of this pair potential was obtained from values for van der Waals radii  $r_i$ , atom polarizabilities  $\alpha_i$ , and the "effective number of electrons"  $N_i$  for each atom type using the Slater-Kirkwood formula for  $c_{ij}$ ; the constants  $a_{ij}$  were assigned to minimize the potential  $E_{ij}$  for the atom pair at an interatomic separation equal to the sum of the van der Waals radii:  $a_{ij} = \frac{1}{2}c_{ij}(r_i + r_j)^6$ . These values were taken from previous works<sup>4,21</sup> and are given in Table II. Throughout this paper, torsion angles are consistently expressed using a right-handed frame of reference, in line with previous convention for descriptions of helical chain conformations.<sup>6,22,23</sup> This is in contrast to much previous work on polypropylene,<sup>4,5,21</sup> where for an isotactic chain the handedness of the frame of reference alternates for successive main-chain torsions. However, this distinction merely requires a change of sign on some torsion angles when comparing results to some literature values.

The conformational energy map for the isolated helical chain calculated in this work using the united methyl atom description is presented in Figure 1. Energy contours up to 5 kcal/mol of the iPP repeat unit, in increments of 1 kcal/mol, are plotted versus the two backbone torsion angles  $\phi_1$  ( $-\text{CH}(\text{CH}_3)\text{CH}_2-$ ) and  $\phi_2$  ( $-\text{CH}_2\text{CH}(\text{CH}_3)-$ ) based on a data grid with increments of  $10^\circ$  in  $\phi_1$  and  $\phi_2$ . (Traditionally,<sup>4,5,21</sup> these torsion angles are labeled  $\phi_i$  and  $\phi_{i+1}$ , respectively, in describing chains with irregular conformations, where the assignment of torsion pairs may differ along the length of the chain.) An essentially identical set of energy contours was obtained using the explicit description of the methyl moiety, in which case the torsion angles describing rotation of the pendant methyl groups were varied in order to obtain the conformation

Table III  
Single-Chain Conformational Energy Minima

minimum <sup>a</sup>	$\varphi_1$ , deg	$\varphi_2$ , deg	energy, <sup>b</sup> kcal/mol	helix twist $\theta_h$ , <sup>c</sup> deg	helix pitch $d_h$ , <sup>c</sup> Å
gt	120	5	0.0	122	2.20
gg	-128	-114	2.2	172	1.86
tt	26	-10	2.9	17	0.98
tg	26	115	2.9	127	2.28
g*g	79	113	3.5	156	2.20

<sup>a</sup> Refer to Figure 1 and ref 4. <sup>b</sup> Units are expressed in kcal/mol of propylene repeat units. <sup>c</sup> Units are expressed per monomeric unit.

of minimum energy for a given set  $\{\varphi_1, \varphi_2\}$ . The locations and energies of the five minima (relative to the lowest energy minimum) corresponding to right-handed helices are listed in Table III; by symmetry, six additional minima represent the corresponding left-handed helices. Previously established nomenclature<sup>4</sup> for the minima is used.

By comparison, the work of Wright and Taylor<sup>6</sup> demonstrates a qualitatively similar set of energy contours, from which these investigators deduced six unique minima, all within 1 kcal/mol of the minimum energy conformation; four of these correlate well in location with the minima suggested here. One additional minimum reported by Wright and Taylor occurs as a shoulder in the broad potential energy well near gt, at roughly  $\{110^\circ, -20^\circ\}$ , and may be traced to the omission of the intrinsic torsional potential about the C-C skeletal bond in their force field. Suter and Flory calculated energy contour maps for irregular chain conformations of both meso and racemic diads of polypropylene using a model in which the atoms of the methyl moiety are explicitly represented. Again, agreement is obtained in the approximate locations of four of the six minima. An additional minimum in the vicinity of  $g^*g = \{70^\circ, -120^\circ\}$  appears in their plots as a result of the conformational freedom enjoyed by diads in irregular chain conformations, made possible by independent rotation of the torsions about successive skeletal bonds. In keeping with the assumption of helical periodicity along the polymer chain and using the single repeat unit as the simplest irreducible structural unit, we have required successive torsion pairs to be equal, which precludes the occurrence of minima in this region of the energy contour plot. Unique to this work is the appearance of a new minimum at  $gg = \{114^\circ, 128^\circ\}$ , which was not observed in previous calculations.

**Crystal Packing.** We have previously presented a method for describing the general construction of a model of the ordered polymer solid state.<sup>22</sup> This construction proceeds by packing of molecular helices on a regular lattice. The fundamental parameters for constructing the ordered phase geometry are the displacement vectors locating equivalent points on neighboring molecules surrounding the parent chain. In this way, the  $\alpha_1$ -modification of iPP is easily described using two equivalent, interpenetrating lattices of right-handed and left-handed helices. This is illustrated in Figure 2. The location of chains within each lattice is specified in terms of  $A$  and  $B$ , the scalar distances from a point on the reference chain to equivalent points in two neighboring chains on the lattice, and the Euler angles,  $\tau$ ,  $\nu$ , and  $\zeta$  defining the orientation of these displacements with respect to the alignment direction of the polymer chains, which projects perpendicularly out of the plane of the page in Figure 2.  $\tau$  is the angle between  $B$  and the alignment direction  $C$  (the direction of the helix axes),  $\nu$  is the angle between  $A$  and  $C$ , and  $\zeta$  is the angle between  $A$  and  $B$ . The second lattice, composed of chains which are mirror images to those in the first lattice, is displaced

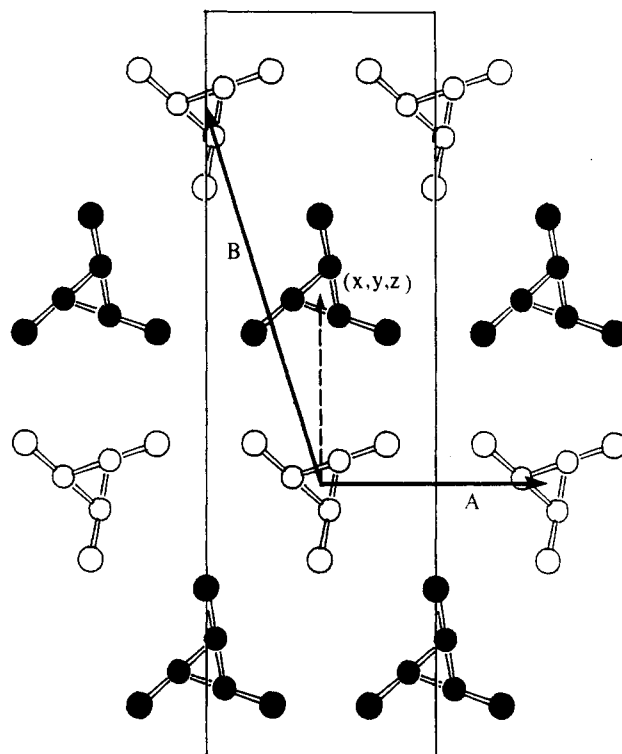


Figure 2.  $\alpha_1$ -Modification of crystalline isotactic polypropylene, as viewed down the  $c$ -axis of the unit cell. The primitive lattice described by the vectors  $A$  and  $B$ , with  $C$  oriented orthogonally to the plane of the paper, used to model the structure, is overlaid. The displacement of the two interpenetrating lattices of right-handed and left-handed chains is described by the vector  $(x, y, z)$ .

Table IV  
Model Lattice Parametrization

$A, B, C$ (Å)	6.65, 10.99, 6.50
$\tau, \nu, \zeta$ (deg)	87.2, 99.3, 107.6
fractional displacement of second lattice $(x, y, z)$	$(1/4, 1/2, -1/2)$

by fractional components  $(x, y, z)$  in the  $A$ ,  $B$ , and  $C$  directions, respectively. Parameters required for this definition of the lattice are provided in Table IV.

We have not considered it necessary to evaluate energies throughout the entire parameter space in this analysis of multichain packing, since we are only interested in the minimum energy structure in the vicinity of the experimentally observed  $\alpha_1$ -modification. A cursory analysis of MM methods of the potential energy surface in the vicinity of the crystalline structure, deduced from extensive experimental evidence, of the  $\alpha_1$ -modification of iPP confirms the stability of this geometry from a potential energy perspective. We allow the following parameters to participate in the energy minimization trajectory: the two chain torsions describing the repeat unit structure; the lattice parameters  $A$ ,  $B$ ,  $\tau$ ,  $\nu$ , and  $\zeta$ ; the lattice shift vector  $(x, y, z)$ , in fractional form; the setting angles  $\omega_1$  and  $\omega_2$ , corresponding to the angle of rotation of the parent chain in each lattice about its helix axis away from the  $x$ - $z$  plane. We constrain the bond lengths and bond angles within the polymer helix to fixed values; the parent chain of the second lattice (right-handed helices) is generated as the mirror image of the parent chain of the first lattice (left-handed helices) by reflection through the  $x$ - $z$  plane prior to creation of the second lattice. The density is fixed at the experimental value of 0.936 g/cm<sup>3</sup> at ambient temperature. The final results of the potential energy minimization are summarized in Table V.

Table V  
Minimum-Energy  $\alpha_1$ -Modification of iPP

torsion (deg)	C-C $\alpha$ -C-C $\alpha$ ( $\varphi_1$ )	-2
	C $\alpha$ -C-C $\alpha$ -C ( $\varphi_2$ )	-122
Model Lattice Description		
A, B, C <sup>a</sup> (Å)		7.04, 10.31, 6.54
$\tau$ , $\nu$ , $\xi$ (deg)		87.2, 98.9, 107.6
$\omega_1$ , $\omega_2$ (deg)		10.9, -71.0
(x, y, z)		0.32, 0.57, -0.50
Conventional Crystallographic Description		
a, b, c (Å)		7.04, 19.67, 6.54
$\alpha$ , $\beta$ , $\gamma$ (deg)		89.8, 98.9, 92.3
(x, y, z)		0.03, 0.28, -0.50
$E_{\text{coh}}$ (kcal/mol)		5.43

<sup>a</sup> The magnitude of the lattice vector in the chain direction is not an independent parameter but follows from the chain conformation.

Experimental measurements for the cohesive energy of amorphous polypropylene suggest values in the range from 3.32 to 4.16 kcal/mol.<sup>24</sup> Correcting these for the potential energy of melting, which to a good approximation equals the measured enthalpy of melting  $\Delta H_m$  of 2.10–2.61 kcal/mol,<sup>24</sup> yields a range of 5.42–6.77 kcal/mol for the experimental crystal cohesive energy. The calculated cohesive energy  $E_{\text{coh}}$  of the crystalline lattice is 5.43 kcal/mol of iPP repeat units (22.7 kJ/mol), in reasonable agreement with the experimental values.

## Relaxation Mechanisms

**General Classifications.** The “ $\alpha$ -relaxation” in iPP observed by NMR conforms to a characteristic reorientation mechanism which produces a net rotation of the molecular helices about their axes.<sup>2</sup> This rotation appears to proceed by discrete jumps of 120°, which is the net twist attributable to a single repeat unit in the 3<sub>1</sub> helical geometry. This process is therefore consistent with jumps between equivalent positions occupied by the atoms of successive repeat units in the polymer chain packed into the crystal lattice. Two general classes of reorientation processes may be proposed to explain the transition from one set of atom positions within the lattice to an equivalent set displaced by one chemical repeat unit along the chain under the condition of helical symmetry. These two classes may be categorized as *concerted-helix* transitions and *defect-translation* transitions. In the first, an arbitrary chain in a perfect crystal lattice undergoes a displacement, as a whole, which moves every monomeric unit  $a_i$  of the chain from its current position to the position  $a_{i+1}$  simultaneously. This concerted motion does not imply, however, that the chain remain rigid during the transition. In the second class of transitions, a reference chain within an otherwise perfect crystal lattice contains a structural irregularity such that, on one side of the irregularity, each monomeric unit  $a_i$  occupies its proper lattice position while on the opposite side of the irregularity the position  $a_{i+n}$  is occupied by the monomeric unit  $a_{i+m}$ , where  $m \neq n$  (except in the case of a disclination, where the monomeric unit  $a_{i+n}$  occupies its proper position but the helix executes an improper number of turns between  $a_i$  and  $a_{i+n}$ ). As the irregularity moves forward or backward along the chain, atoms previously settled in one lattice position are moved to an equivalent lattice position  $|m-n|$  away. Considerable attention has been directed to these two classes of transitions in crystalline PE.<sup>9–12,25,26</sup> Reneker and Mazur<sup>10</sup> have provided a concise, descriptive classification scheme for transitions of the defect-translation type, which are summarized in Table VI. Here we consider only trapped defect structures within crystals and do not

Table VI  
Classification of Defect-Translation Transition in Regular Helices<sup>a</sup>

defect name	net twist displacement	net pitch displacement
dispirations		
(a) interstitial	$-\theta_h$	$-d_h$
(b) vacancy	$+\theta_h$	$+d_h$
disclination	$\pm N\theta_h$	0
dislocations		
(a) interstitial	0	$-Nd_h$
(b) vacancy	0	$+Nd_h$

<sup>a</sup> Net twist displacement refers to the rotational displacement of the occupied lattice position  $a_{i+m}$  from the undeformed helix position  $a_{i+n}$ ; net pitch displacement refers to the translation along the helix axis between these two positions.  $\theta_h$  and  $d_h$  are the twist and pitch, respectively, per repeat unit in the regular helix.  $N$  is the number of constitutional repeat units per helical repeat unit (i.e., three for the 3<sub>1</sub> helix of isotactic polypropylene).

consider the possible existence and concerted translation of entire defect boundaries between neighboring crystallographic domains.

**Concerted-Helix Transitions.** In this form of molecular motion, all of the atoms of the mobile chain undergo the simultaneous progression from one set of lattice points to another, symmetry-equivalent set of lattice points. Realistically, one must imagine that the initial and final geometries, conforming to ideal crystalline structures, are only the stable end points of the transition trajectory; this does not imply, however, that along the transition path between these end points either the mobile chain (i.e., that undergoing the transition) or the surrounding chains in the lattice necessarily remain fixed in the most stable conformation appropriate to the ideal lattice. As the mobile chain proceeds along its transition trajectory, its interaction with the atoms of neighboring chains will cause a temporary distortion of its own conformation, as well as of the conformations of chains in the nearby environment affected by the motion of the mobile chain. The extent of this “affected domain” is not known a priori. We have considered here the two simplest cases, that of a rigid mobile chain in a rigid lattice and that of a flexible mobile chain in a rigid lattice. In the first case, the mobile chain performs a simple rigid-body translation-rotation within the confines of the surrounding lattice. In the second case, at each point in the translation-rotation operation of the chain displacement, the conformation of the mobile chain is allowed to relax to that which minimizes the total potential energy of the packed structure, subject to the constraint of helical symmetry in the mobile chain. By so doing, we have neglected deformation of the neighboring environment completely.

The potential energy maps for these two cases are shown in Figures 3 and 4. In these plots, the abscissa represents the translation of the reference chain along its helix axis as a fraction of the helix repeat length (i.e., 6.54 Å); the ordinate represents the rotation of the chain helix about its axis, defined by the angle between the vector from the helix center to the first carbon atom and C. The 3-fold symmetry due to the 3<sub>1</sub> symmetry of the lattice cavity is immediately apparent. From the rigid chain/rigid lattice simulations, we deduce a barrier to screw displacement of 5.9 kcal/mol of propylene units; this is in very good agreement with the results of Syi and Mansfield, who obtained a barrier to the {120° rotation,  $c/3$  translation} screw transition of 3–4 kcal/mol main-chain carbons or 6–8 kcal/mol of propylene units. It may be pointed out that we have used the united methyl atom in these calculations, whereas Syi and Mansfield have included

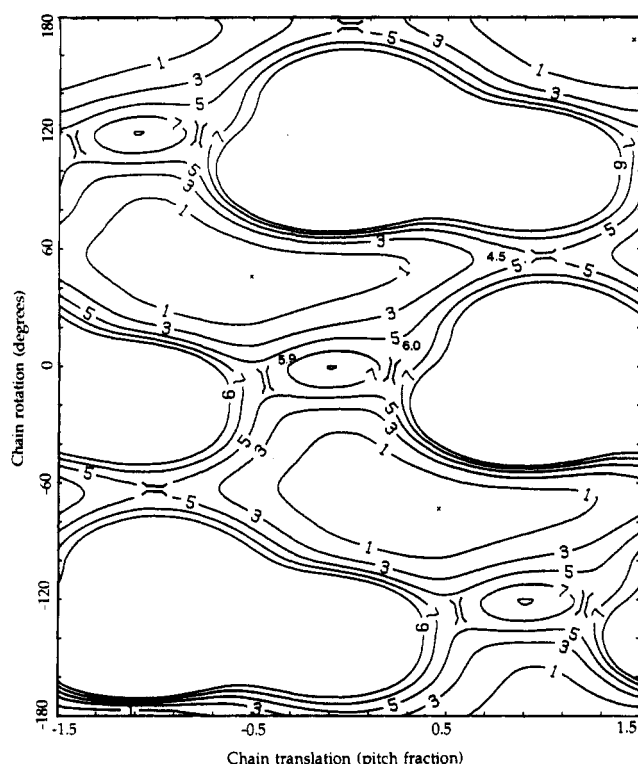


**Figure 3.** Potential energy contour plot for the placement of a rigid  $3_1$  helix of iPP within a rigid lattice of  $\alpha$ -phase crystalline iPP. The 'x's mark the 3-fold symmetric minimum-energy packing. Refer to the text for details.

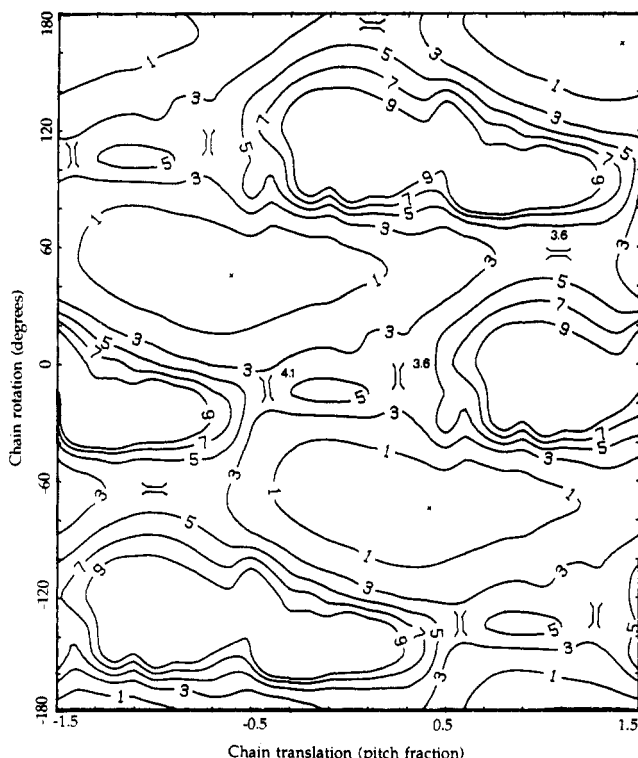


**Figure 4.** Potential energy contour plot for the placement of a flexible (approximately  $3_1$ ) helix of iPP within a rigid lattice of  $\alpha$ -phase crystalline iPP. The 'x's mark the 3-fold symmetric minimum-energy packing. Refer to the text for details.

explicit methyl descriptions. This agreement further supports the conclusion that the results are relatively insensitive to the details of methyl group representation. Furthermore, it is interesting to note that two screw-transition pathways having almost identical barriers exist,

corresponding roughly to the two possible sequences of events: rotation-translation or translation-rotation. The two saddle points are separated by a low maximum which is due to the repulsive interaction of methyl groups with methine hydrogens.

A second viable chain motion which may be deduced from the potential energy map involves simple translation of the chain through the lattice parallel to its helix axis, with a barrier of only 4.5 kcal/mol. This lower barrier would imply that the rate of axial diffusion of iPP chains within the solid state may be higher than that of the screw transitions observed by 2D NMR experiments. Calculations for PE have similarly indicated<sup>8,9,13</sup> that, for concerted-helix transitions, pure translations are favored over screw mechanisms.

From the flexible chain/rigid lattice simulations, it is apparent that the basic features of chain motion remain unchanged. The primary benefit of the increased conformational flexibility is a reduction in each of the transition barrier heights by roughly 1–1.5 kcal/mol of monomeric units. The barrier heights for both screw and translational displacement fall to 3.6 kcal/mol. Permitting the chains in the first neighbor shell in the lattice to participate in the cooperative motion of the mobile chain is likely to produce a further incremental reduction in these potential energy barriers; however, the operative mechanisms are not likely to change and, as will be observed shortly, such incremental changes in energy barriers may play only a minor role in comparison to energies of competing mechanisms in crystallites of realistic thicknesses.

The barrier to concerted-helix motion in the crystal lattice is chain length dependent. Taking a barrier height to a screw displacement of roughly 3.6 kcal/mol of repeat units, an activation energy of 43–68 kcal/mol, on the order of activation energies deduced experimentally,<sup>2</sup> would entail motion of a chain segment 20 to 38 carbon atoms long for a  $\{-120^\circ, c/3\}$  transition. This may only be possible in a crystallite of lamellar thickness 40 Å or less. Experimental determinations of lamellar thickness, based on the long period observed in small-angle X-ray scattering, typically fall in the range from 120 to 300 Å, depending upon the temperature and processing conditions imposed during crystallization.<sup>27,28</sup>

**Defect-Translation Transitions.** The alternative to concerted-helix motion of a chain within a crystal, which leads inevitably to a chain length-dependent activation energy and by extension to an activation energy which is a linear function of lamellar thickness, is that of a mobile "metastable state", or defect structure. Characterization of such an activated process would entail two components. The first is the estimation of the energy of formation and the stability against dissipation of the metastable state within the crystalline phase; the second is the barrier limiting translation of the metastable state through the crystal structure. The former of these is addressed in the following section via a MM approach. We do not propose here to categorically define the sole structure of the defect state within the iPP  $\alpha$ -crystalline phase; it is quite likely that the detailed geometries of defect structures will vary widely, so long as they satisfy, over some finite section of the chain, the restriction of crystal lattice occupancy from the boundaries of the defect segment outward into the regular crystalline phase and the constraints of the "tube" defined by the neighboring lattice chains.

The estimation of barriers to translation requires the determination of the transition-state energy between symmetrically equivalent metastable states, either by a

molecular dynamics approach or by a quasi-static molecular mechanics approach. Detailed molecular dynamics simulations is precluded by the long time scale<sup>2</sup> of this transition process, which exceeds that accessible by current molecular dynamics methods.

Molecular mechanics, on the other hand, relies on the introduction of any one viable representative from a very large number of essentially arbitrary candidates into the otherwise perfect crystalline structure and additionally the characterization of an almost indeterminate number of possible transition trajectories between metastable states. A comprehensive treatment of the latter problem is clearly beyond the scope of this paper.

One practical solution would be to limit the search to rotational isomeric state (RIS) conformers; this could reduce the set of inspected states for a short segment of the polymer chain to a reasonably small and tractable size. To this end, we scanned all possible RIS conformers of the finite-length iPP segment, subject to the following constraints: (a) all main-chain carbons fit within a cylindrical cavity of diameter 6.08 Å concentric with the 3<sub>1</sub> polymer helix; (b) the end-to-end vector of the RIS segment connects the two uniform 3<sub>1</sub> helices in their respective (i.e., displaced) lattice positions within a precision of 0.1 Å; (c) the transformation matrix describing the orientation of the second helix relative to the first is commensurate with the proposed defect geometry to within 10% in any element of the matrix. We considered both three-state<sup>29</sup> and five-state<sup>4</sup> RIS schemes, the former in segments up to nine repeat units long and the latter in segments up to five repeat units long. This approach revealed several conformers consistent with a disclination defect model. However, in order to explain the helix jump behavior in the NMR data of iPP, only dispirations are suitable; dislocations and disclinations, when traveling as defects along helical rods, will not produce spectroscopically-recognizable net angular twists about the helix axis. Unfortunately, this approach suggested that there are no RIS chain conformations which fit within the crystal channel and at the same time are commensurate with either the interstitial or vacancy-type dispiration. This situation is analogous to that found for polypropylene chains confined to a channel in a clathrate crystal.<sup>30</sup>

We propose instead to identify at least one viable defect structure which satisfies the aforementioned criteria and is consistent with experimental observation, thereby establishing the validity of the mechanism. As (stable) defect structures we envision conformations of chain segments connecting two segments of regular 3<sub>1</sub> helices in a perfect lattice register such that the potential energy of the total system is in a local minimum. The identification of an appropriate initial guess for the metastable state may be greatly simplified by examination of the energies of the isolated chain conformations. For any number of repeat units to be included in the metastable state, one may calculate the two main-chain torsions required to satisfy the lattice occupancy restrictions of the integral defect transition under the assumption that the defect segment itself is a segment of a uniform helix.

In the vacancy-type dispiration, one requires at least 12 repeat units in a uniform helix to span the extra distance produced by the displacement  $+d_h$  (see Table VI). The single-chain potential energy of this dispiration decreases asymptotically toward the undeformed chain energy as the dispiration is distributed over an increasing number of repeat units. In the potential energy map in Figure 1, a point representing the chain conformation of the deformed (right-handed) helix would start at the location

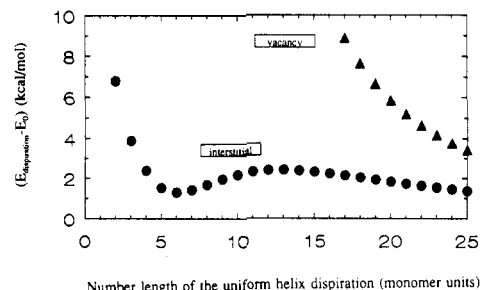


**Figure 5.** Excess conformational energies (above that of the regular iPP 3<sub>1</sub> helix) of uniform helices describing a net dispiration in the iPP 3<sub>1</sub> helix, either interstitial type  $\{-120^\circ, -c/3\}$  or vacancy type  $\{+120^\circ, +c/3\}$ , as functions of the number of propylene units participating in the dispiration. Energy values are given per mole of constitutional repeat units.

$\{92^\circ, 66^\circ\}$  for  $n = 12$  and converge to the most stable state at  $\{120^\circ, 5^\circ\}$  as the number of repeat units participating in this type of dispiration increased. Figure 5 illustrates the dependence of the excess chain conformation energy of the helix describing a uniformly-distributed defect as a function of the number of propylene units participating in the dispiration.

In the interstitial-type dispiration, where extra monomer units are effectively crowded into the crystal between two helical segments in the lattice register, a point representing the deformed (right-handed) helix starts at the location  $\{66^\circ, -37^\circ\}$  in Figure 1 and encounters a minimum in energy as the number of monomeric units contained in the deformed helix increases; Figure 5 indicates that the minimum in the curve of potential energy versus dispiration length  $n$  occurs at  $n = 6$ , followed by a maximum at  $n = 13$  and a subsequent asymptotic decrease in energy with increasing  $n$ . The interstitial dispiration for  $n = 6$  is described by the main-chain torsions  $\{\varphi_1, \varphi_2\} = \{110^\circ, -30^\circ\}$ . The different behaviors of the conformational energies of the uniformly-distributed dispirations of the vacancy and interstitial types might be interpreted to mean that a "tensile solitary wave" (i.e., vacancy-type dispiration) is unstable in an iPP crystal and will be dissipated through the crystal surfaces, while a "compressive solitary wave" (i.e., interstitial-type dispiration) may be stable and able to propagate reversibly. It may also be noted that the conformational minimum at  $\{79^\circ, 113^\circ\}$  (i.e.,  $g^*g$ ) is a close approximation to a disclination distributed evenly over nine repeat units. These are the lowest energy conformations which satisfy the criteria for defects which are commensurate with the lattice and which are stable, in a minimum potential energy sense, against dissipation of the defect over the entire length of the polymer chain.

Viable metastable state structures in long iPP chains were determined by first replacing a segment of a chain in the lattice by one of the stable uniform deformation helices, e.g., the six-repeat dispiration. The initial chains so generated were then allowed to assume conformations of minimum intramolecular potential energy under the imposition of the respective defect-type (e.g., dispiration) constraints; one repeat unit on either end of the defect was allowed to participate, along with the  $n$  repeat units of the defect segment itself, in the minimization process. Helical symmetry was no longer enforced at this stage. This initial step ensured a sufficiently linear chain for insertion into the regular lattice. Each defect state segment was then allowed to come to a minimum total potential energy packed in the regular lattice of the  $\alpha$ -crystalline form. Figure 6 illustrates this process for the generation of a defect structure. Shown are segments of the undistorted 3<sub>1</sub> helix, the isolated chain with insertion



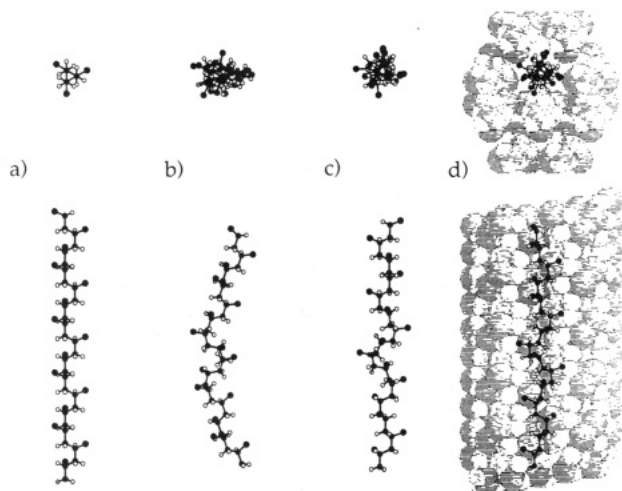


**Figure 6.** Illustration of the evolution of a chain conformation in the generation of metastable defect geometries: (a) the undistorted  $3_1$  iPP helix; (b) the same chain after insertion of a six-repeat dispiration in the central portion of the chain; (c) the minimum-energy conformation of the isolated chain subject to dispiration end constraints; (d) the final conformation of the minimum-energy dispiration within the crystal lattice.

of the  $n$  unit defect state initial guess, the same chain after the single-chain "relaxation", and the final defect structure after minimization within the confines of the crystal lattice. For the sake of computational expediency, bond lengths and bond angles were held fixed and only main-chain torsions over the central  $n + 2$  repeat unit segment were allowed to participate in the energy minimization. Thus the dispiration suggested by the uniformly-distorted helix was realized allowing 16 degrees of freedom. During energy minimization, candidate chains were anchored in the lattice at both ends using rigid  $3_1$  helix segments five repeat units long.

The excess potential energy of the above-determined metastable states was deduced from the linear dependence of the lattice energy as a function of chain length. The total energy per repeat unit,  $E_{\text{total}}$ , of the structure decreases linearly as a function of the inverse of the total length  $N$  of the chain,  $E_{\text{total}} = (n + 2)E_{\text{excess}}/N + E_{\text{lat}}$ , where  $E_{\text{lat}}$  is the per repeat unit energy of the perfect lattice and  $E_{\text{excess}}$  is the per repeat unit excess energy for the  $n + 2$  repeat units participating in the localized defect within the lattice;  $(n + 2)E_{\text{excess}}$  represents the energy of formation of the metastable state. We determine a formation energy of 23.4 kcal/mol (97.9 kJ/mol) of defects for the most stable dispiration defect structure.

The defect formation energy may be further subdivided into its component contributions due to intramolecular distortion and intermolecular packing interactions. For the dispiration considered, the intramolecular contribution per defect is 11.2 kcal/mol (46.9 kJ/mol), 9.5 kcal/mol (38.5 kJ/mol) of which is due to bond torsions and 1.7 kcal/mol (7.1 kJ/mol) of which is due to nonbonded intramolecular interactions. The remaining 12.2 kcal/mol (51.0 kJ/mol) is intermolecular in origin, suggesting that, at least in this instance, the energy required to accommodate the defect structure is evenly split among distortions of intramolecular conformation and intermolecular packing. Other defect structures considered by us exhibited comparable intermolecular contributions to the potential energy but similar or larger intramolecular contributions due to bond torsion distortion. This large variance in intramolecular contributions to the energy of formation of defects underscores the importance of low defect conformational energy in achieving reasonable geometries and emphasizes

the selectivity of the metastable state in favor of energetically-competitive chain conformers.

## Conclusion

Experimental evidence has suggested that the  $\alpha$ -relaxation in iPP is related to a single process consisting of  $120^\circ$  jumps of the chain helix about its axis within the crystalline phase of the bulk polymer. Two mechanisms which are consistent with these observations are concerted-helix transitions, in which entire helices move cooperatively, and defect-translation transitions, in which a defect structure passing as a solitary wave along a chain produces sequential rotation of segment groups within the chain. An attempt to clarify these two mechanisms through explicit modeling of the crystal structure and the energies involved in such transitions suggests that, in the former case, the concerted-helix transition, the requisite activation energy is on the order of 3.6 kcal/mol of repeat units and should increase linearly with crystal thickness. Experimentally observed activation energies limit this type of motion to crystallite thicknesses of 40 Å or less, making this mechanism improbable in realistic circumstances.

The alternative case, involving the existence of a localized dispiration, requires as little as 23.4 kcal/mol of defects, which makes it energetically advantageous to the concerted-helix transition in most crystallites of realistic thicknesses. In the event that the dispirations behave as free-streaming entities (i.e., in the absence of additional barriers to motion of the dispiration along the chain) the balance between the formation energy of 23.4 kcal/mol and the experimental activation energy of 45–70 kcal/mol may be attributable to the kinetic energy of these defects themselves. Where the dispirations must pass through higher energy (saddle point) conformations (relative to the stable static dispiration considered here), the motion may be thought of as an activated process transforming metastable static dispirations into neighboring but otherwise similar defects, with a supplemental activation energy of defect motion over and above the energy of defect formation. In similar calculations for PE<sup>9,11</sup> supplemental activation energies on the order of 4–17 kcal/mol have been determined; similar values for iPP, in combination with the calculated energy of formation, would be well within the range of credible magnitudes required by the experimental data. Consideration of likely static defect structures in iPP suggests that in fact the intermolecular packing forces are relatively insensitive to the exact nature of the defect structure, whereas intramolecular forces are quite sensitive and may effectively select between alternative defect geometries.

Finally, as an aside, we note that the 2D NMR experiments that provided the stimulus for these calculations<sup>2</sup> are insensitive to dislocations. For this reason we have not considered further the concerted-helix axial translation mechanism described above, even though it is a process of low activation energy. However, experiments that prove that polymer chains can diffuse in and out of polymer crystals<sup>31</sup> are available, at least for PE; in such cases there is no need to disregard such mechanisms not involving net rotations. Comparing the measured activation energy of chain diffusion (25.1 kcal/mol, or 105 kJ/mol) with the available calculated values<sup>8,13</sup> of activation energy of 0.3–0.5 kcal/mol methylene groups in a concerted-helix translation in PE makes it immediately clear that for lamellae in excess of 100 Å thickness a concerted-helix mechanism is not likely. Rather, a succession of crystallographic defects of the dislocation type could also account for such translational displacements, similar to the role

played by dispirations in effecting rotational displacements.

**Acknowledgment.** This work was supported by financial assistance from the Schweizerische Nationalfonds zur Foerderung der Wissenschaftlichen Forchung (NF Sektion II). We thank Professor H. W. Spiess for providing us with the manuscript of ref 31 prior to publication.

## References and Notes

- (1) Boyd, R. H. *Polymer* **1985**, *26*, 323-347.
- (2) Schaefer, D.; Spiess, H. W.; Suter, U. W.; Fleming, W. W. *Macromolecules* **1990**, *23*, 3431-3439.
- (3) Abe, A.; Jernigan, R. L.; Flory, P. J. *J. Am. Chem. Soc.* **1966**, *88*, 631-639.
- (4) Suter, U. W.; Flory, P. J. *Macromolecules* **1975**, *8*, 765-776.
- (5) Yoon, D. Y.; Sundararajan, P. R.; Flory, P. J. *Macromolecules* **1975**, *8*, 776-783.
- (6) Wright, N. F.; Taylor, P. L. *Polymer* **1987**, *28*, 2004-2008.
- (7) Tashiro, K.; Kobayashi, M.; Tadokoro, H. *Macromolecules* **1977**, *10*, 731-736.
- (8) McCullough, R. L. *J. Macromol. Sci., Phys.* **1974**, *B9*, 1, 97-139.
- (9) Mansfield, M.; Boyd, R. H. *J. Polym. Sci., Part B: Polym. Phys.* **1978**, *16*, 1227-1252.
- (10) Reneker, D. H.; Mazur, J. *Polymer* **1988**, *29*, 3-13.
- (11) Reneker, D. H.; Fanconi, B. M.; Mazur, J. *J. Appl. Phys.* **1977**, *48*, 4032.
- (12) Reneker, D. H.; Mazur, J. *Polymer* **1982**, *23*, 401-412.
- (13) Syi, J.-L.; Mansfield, M. L. *Polymer* **1988**, *29*, 987-997.
- (14) Bleha, T.; Gajdos, J.; Karasz, F. E. *Macromolecules* **1990**, *23*, 4076-4082.
- (15) Natta, G.; Corradini, P. *Nuovo Cimento* **1960**, *15*, Series X (supplement), 40-51.
- (16) Turner-Jones, A.; Aizlewood, J. M.; Beckett, D. R. *Makromol. Chem.* **1964**, *75*, 134-158.
- (17) Gomez, M. A.; Tanaka, H.; Tonelli, A. E. *Polymer* **1987**, *28*, 2227-2232.
- (18) Mencik, Z. *J. Macromol. Sci., Phys.* **1972**, *B6*, 101-115.
- (19) Hikosaka, M.; Seto, T. *Polym. J.* **1973**, *5*, 111-127.
- (20) Napolitano, R.; Pirozzi, B.; Varriale, V. *J. Polym. Sci., Phys.* **1990**, *28*, 139-147.
- (21) Theodorou, D. N.; Suter, U. W. *Macromolecules* **1985**, *18*, 1467-1478.
- (22) Rutledge, G. C.; Suter, U. W. *Macromolecules* **1991**, *24*, 1921-1933.
- (23) Miyazawa, T. *J. Polym. Sci.* **1961**, *55*, 215-231.
- (24) Van Krevelen, D. W. *Properties of Polymers*; Elsevier: New York, 1972.
- (25) Boyd, R. H. *Polymer* **1985**, *26*, 1123-1133.
- (26) Van der Werff, H.; van Duynen, P. T.; Pennings, A. J. *Macromolecules* **1990**, *23*, 2935-2940.
- (27) Samuels, R. J. *J. Polym. Sci., Polym. Phys. Ed.* **1968**, *6*, 2021-2041.
- (28) Maeda, Y.; Nakayama, K.; Kanetsuna, H. *Polym. J.* **1982**, *14*, 295-304.
- (29) Flory, P. J. *Statistical Mechanics of Chain Molecules*; Hanser: Munich, 1989.
- (30) Tonelli, A. E. *Macromolecules* **1991**, *24*, 3069-3073.
- (31) Schmidt-Rohr, K.; Spiess, H. W. *Macromolecules* **1991**, *24*, 5288-5293.

**Registry No.** iPP (isotactic homopolymer), 25085-53-4.